

3  
4 **Running title:** Role of miR-5681b/Beclin-1 in PCa

5  
6 **The miR-5681b/Beclin-1 axis regulates tumor autophagy to affect the proliferation and**  
7 **apoptosis of prostate cancer cells**

8  
9 Yanmei Zhang, Jiaojiao Li, Quan Li, Yuan Cao\*

10  
11 Department of Clinical Laboratory, The First Affiliated Hospital of Xi'an JiaoTong University  
12 Yulin Hospital, Yulin, Shaanxi, China

13  
14 \*Correspondence: caoyuann22@163.com

15  
16 **Received June 19, 2025 / Accepted April 8, 2026**

17  
18 Prostate cancer (PCa) is a leading cause of cancer-related mortality among men. This study aims to  
19 investigate the regulatory effect of microRNA (miR)-5681b, a potential upstream miR of Beclin-1,  
20 on PCa cell proliferation and apoptosis. Two PCa cell lines (PC3 and LnCaP cells) with relatively  
21 low miR-5681b expression were treated with miR-5681b mimic, pcDNA3.1-Beclin-1, or an  
22 autophagy activator Rapamycin. A xenograft tumor model was established in nude mice, and the  
23 tumor-bearing mice were treated with agomir miR-5681b. The levels of miR-5681b, Beclin-1  
24 mRNA, and apoptosis- and autophagy-associated proteins were evaluated using western blot and  
25 RT-qPCR. The binding between Beclin-1 and miR-5681b was testified by dual-luciferase reporter  
26 gene assay. Cell biological behaviors, as well as Ki-67-positive cells and apoptosis in mouse tumor  
27 tissues, were examined. The results showed that miR-5681b was downregulated in PCa cells and  
28 targeted Beclin-1. miR-5681b overexpression in PCa cells significantly suppressed cell  
29 proliferation and B-cell lymphoma 2 (Bcl-2) levels while augmenting cell apoptosis and the levels  
30 of Bcl-2-associated X (Bax) and cleaved caspase-3. Importantly, miR-5681b inhibited PCa cell  
31 proliferation and autophagy but promoted PCa cell apoptosis, whereas Beclin-1 upregulation  
32 reversed these effects. Activating autophagy also reversed miR-5681b-regulated proliferation and  
33 apoptosis of PCa cells. *In vivo*, miR-5681b overexpression inhibited PCa tumor growth by  
34 modulating the Beclin-1-mediated autophagy pathway. Collectively, these findings suggested that  
35 miR-5681b was lowly expressed in PCa cells, and miR-5681b overexpression inhibited autophagy  
36 by targeting Beclin-1, thereby suppressing the growth of PCa.

37  
38 **Key words:** miR-5681b; Beclin-1; prostate cancer; autophagy; proliferation; apoptosis; autophagy  
39 agonists; rapamycin

42 Prostate cancer (PCa) is one of the most common non-cutaneous malignancies in men, and its  
43 incidence has been rising significantly in the Asian population [1, 2]. The prevalence of PCa  
44 increases with age, and the risk of developing the disease becomes substantially higher in older  
45 individuals [3]. The progression of prostate malignancy involves multiple stages, beginning with  
46 prostate intraepithelial neoplasia (PIN), advancing to localized PCa, subsequently evolving into  
47 advanced prostate adenocarcinoma with local invasion, and ultimately inducing metastasis [4]. PCa  
48 can be classified as androgen-sensitive or androgen-insensitive based on its response to testosterone  
49 stimulation, which directly influences therapeutic strategies [5]. Current treatment options include  
50 active surveillance, radiotherapy, chemotherapy, hormone therapy, cryotherapy, and surgery [6].  
51 Despite advances in clinical management, PCa continues to pose major challenges, including  
52 overtreatment of essentially benign lesions and limited therapeutic options for metastatic disease  
53 [7]. Therefore, further research into the mechanisms underlying PCa is essential for identifying new  
54 therapeutic targets.

55 Autophagy is a key intracellular process responsible for the degradation and recycling of damaged  
56 molecules [8]. It occurs frequently during tumorigenesis and cancer chemotherapy. Functional  
57 autophagy can protect cancer cells from chemotherapy-induced cytotoxicity, contributing to  
58 treatment resistance and refractory diseases [9]. Beclin-1, the first essential autophagy-related  
59 protein discovered, is critically involved in the development of several cancers when deleted or  
60 impaired [10]. Studies have demonstrated that Beclin-1 regulates multiple pathways, including  
61 mTOR, PI3K/AKT, and p53, thereby influencing cell development and viability [11-13]. Given the  
62 close relationship between autophagy and apoptosis, autophagy can influence the sensitivity of PCa  
63 cells to chemotherapy and radiation [14]. In addition, Beclin-1 can interact with microRNAs  
64 (miRNAs) to modulate autophagy in tumor cells. For example, miR-93 interacts with Beclin-1 to  
65 regulate autophagy in glioblastoma, affecting tumorigenicity and treatment resistance [15].  
66 Knockdown of Beclin-1 inhibits autophagy and induces apoptosis in BPH-1 cells [16]. However,  
67 the relevant upstream mechanisms of Beclin-1 involving miRNAs in PCa have not been fully  
68 elucidated.

69 miRNAs are defined as a type of non-coding RNA molecule with a length of roughly 21-25  
70 nucleotides, which are widely present in eukaryotic cells [17]. miRNAs play a critical regulatory

71 function in cellular processes and exert influence over the translation efficiency and stability of  
72 mRNA molecules through their interaction with the 3'-untranslated region (3'-UTR) of the target  
73 mRNA, thereby governing gene expression [18]. miRNAs are pivotal regulators in a wide range of  
74 biological processes, including cell apoptosis, growth, and metabolism [17]. Notably, the  
75 significance of miRNAs in the occurrence and progression of PCa has been extensively  
76 investigated and acknowledged in academic research. For instance, miR-21 is overexpressed in  
77 PCa and is recognized as a promoting factor that enhances cellular viability and proliferation while  
78 suppressing programmed cell death [19]. Conversely, several miRNAs, such as miR-34a and  
79 miR-129-5p, have been observed to impede the growth and spread of PCa cells while promoting  
80 apoptosis [20, 21]. Accordingly, a thorough analysis of PCa-associated miRNAs is necessary to  
81 identify novel PCa-related miRNAs and their corresponding target genes, which is instrumental in  
82 elucidating new molecular targets and devising individualized treatment strategies. In this study, we  
83 obtained downregulated miRNAs in PCa patients from the dbDEMC database, PCa-related  
84 miRNAs from the GeneCards database, and upstream miRNAs of Beclin-1 from the miRanda  
85 database. The intersection of the results of these three datasets yielded the unique candidate,  
86 miR-5681b, which was selected as the research subject. Nonetheless, to date, there have been no  
87 literature reports on the expression pattern and mechanism of miR-5681b in malignant tumors.  
88 Surprisingly, preliminary evidence suggests that miR-5681b can inhibit the proliferation of vascular  
89 smooth muscle cells [22], suggesting that miR-5681b may influence cellular phenotypes by  
90 regulating cell proliferation. Uncontrolled and excessive cell division and proliferation can lead to  
91 the formation of malignant tumors [23]. Therefore, we hypothesized that miR-5681b may influence  
92 PCa cell autophagy by targeting and inhibiting Beclin-1 expression, thereby affecting PCa cell  
93 proliferation and apoptosis. A detailed investigation into the relationship between miR-5681b,  
94 Beclin-1, and autophagy in PCa cells may offer new insights for developing targeted therapeutic  
95 strategies. This study may help clarify the molecular mechanisms underlying autophagy regulation  
96 in PCa progression and provide a theoretical foundation for novel anticancer treatments.

97

## 98 **Materials and methods**

99 **Ethics statement.** All animal experiments were reviewed and approved by the Institutional Animal  
100 Care and Use Committee of The First Affiliated Hospital of Xi'an JiaoTong University Yulin  
101 Hospital. Significant efforts were made in order to minimize both the number of animals used and  
102 their respective suffering.

103 **Bioinformatics analysis.** LogFC > 2 and FDR < 0.05 were introduced as filter criteria to choose  
104 the differential miRNAs in PCa patients downloaded from the dbDMEC 3.0 database  
105 (<https://www.biosino.org/dbDEMC/index>) (GSE112264, EXP00622; serum samples of 809 patients  
106 with PCa, 241 negative prostate biopsies, 500 patients with other cancer types were obtained from  
107 the National Cancer Center in Japan, and serum samples of 41 healthy control samples were  
108 acquired from two other hospitals in Japan). The differential gene volcano map was plotted by the  
109 R package “ggplot2”. The miRanda database (<https://mirdb.org/>) and the Genecards database  
110 (<https://www.genecards.org/>) were employed to identify potential upstream miRNAs of Beclin-1  
111 and PCa-related miRNAs, respectively. The intersection of these three databases identified  
112 miR-5681b as the sole candidate for further investigation.

113 **Cell culture.** The human normal prostate epithelial cell line RWPE-1 and PCa cell lines (DU145,  
114 PC3, LnCaP, and 22RV1) were obtained from BeNa Culture Collection (Beijing, China). RWPE-1  
115 cells ( $2.5 \times 10^5$ ) were seeded in Dulbecco's modified Eagle medium (Sigma, St. Louis, MO, USA)  
116 using 24-well plates, while PCa cell lines ( $2.5 \times 10^5$ ) were seeded in Roswell Park Memorial  
117 Institute 1640 medium (Sigma) comprising 10% fetal bovine serum (Sigma), followed by cell  
118 culture in a humidified incubator at 37 °C with 5% CO<sub>2</sub>.

119 **Cell transfection and grouping.** Mimic negative control (NC), miR-5681b mimic, pcDNA3.1  
120 empty vector, and pcDNA3.1-Beclin-1 were transfected into PC3 and LnCaP cells using  
121 Lipofectamine 2000 (Invitrogen, Carlsbad, CA, USA) according to the manufacturer's instructions.  
122 The final concentrations were 50 nM for mimic NC and miR-5681b mimic and 100 nM for the  
123 pcDNA3.1 empty vector and pcDNA3.1-Beclin-1. All transfected materials were obtained from  
124 GenePharma (Shanghai, China). Subsequent experiments were performed 48 h following cell  
125 transfection.

126 Cells were grouped as follows: 1) Blank group; 2) mimic NC group: PC3 and LnCaP cells were  
127 introduced with mimic NC; 3) miR-5681b mimic group: PC3 and LnCaP cells were delivered with

128 miR-5681b mimic; 4) miR-5681b mimic+pcDNA group: PC3 and LnCaP cells were co-transfected  
129 with miR-5681b mimic and pcDNA3.1 empty vector; 5) miR-5681b mimic+pcDNA-Beclin-1  
130 group: miR-5681b mimic and pcDNA3.1-Beclin-1 were co-transfected into PC3 and LnCaP cells; 6)  
131 miR-5681b mimic+Rapamycin group: PC3 and LnCaP cells were delivered with miR-5681b mimic  
132 and concomitantly treated with 50 mM of an autophagy activator Rapamycin (Sigma) for a  
133 duration of 24 hours [24]; 7) miR-5681b mimic+DMSO group: PC3 and LnCaP cells were treated  
134 with miR-5681b mimic and while being treated with 50 mM dimethyl sulfoxide (DMSO; Sigma)  
135 for 24 h.

136 **Reverse transcription quantitative polymerase chain reaction (RT-qPCR).** Total RNA was  
137 extracted from samples using the TRIzol reagent (Invitrogen). RNA concentration and quality were  
138 assessed with a NanoDrop 2000 (Thermo Fisher Scientific Inc., Waltham, MA, USA), and  
139 complementary DNA was then synthesized. mRNA was reverse-transcribed using the  
140 SuperScript™ III Reverse Transcriptase Kit (Invitrogen), and miRNA was reverse-transcribed  
141 using the miRCURY LNA RT Kit (Qiagen, Duesseldorf, Germany). RT-qPCR was carried out  
142 using THUNDERBIRD SYBR® qPCR Mix (Toyobo, Osaka, Japan). RNA relative expression was  
143 calculated using the  $2^{-\Delta\Delta Ct}$  method. Glyceraldehyde-3-phosphate dehydrogenase (GAPDH) was  
144 used as the mRNA internal reference gene, and U6 served as the internal reference gene for miRNA  
145 [25]. The amplified primer sequences of each gene and its primer are detailed in F1.

146 **Dual-luciferase reporter gene assay.** The targeted binding sites between miR-5681b and Beclin-1  
147 were predicted by the MiRanda database (<https://mirdb.org/>). Complementary binding sequences  
148 and mutant sequences of miR-5681b and Beclin-1 were amplified and cloned into a pmiR-GLO  
149 luciferase vector (Promega, Madison, WI, USA) to construct wild-type (Beclin-1-WT) and mutant  
150 (Beclin-1-MUT) reporter plasmids. Thereafter, Beclin-1-WT or Beclin-1-MUT was then  
151 co-transfected with mimic NC and miR-5681b mimic (GenePharma) into PC3 and LnCaP cells  
152 using Lipofectamine™ 2000 (Invitrogen) according to the manufacturer's instructions. Luciferase  
153 activity was evaluated 48 h after transfection.

154 **Cell counting kit-8 (CCK-8) assay.** Cell viability was assessed using a CCK-8 kit (Solarbio,  
155 Beijing, China). Briefly, cells were seeded in 96-well plates ( $5 \times 10^4$  cells/well) and incubated  
156 overnight with 5% CO<sub>2</sub> at 37 °C. Subsequently, 10 µl of CCK-8 reagent was added to each well and

157 incubated for 2 h. Absorbance was measured at 450 nm under a microplate reader (BioTek,  
158 Winooski, VT, USA).

159 **5-ethynyl-2'-deoxyuridine (EdU) staining.** Cell proliferation was evaluated using the EdU Stain  
160 Proliferation Kit (Abcam, Cambridge, UK). Cells were incubated with EdU solution under optimal  
161 growth conditions for 24 h, washed, and then fixed with the fixative solution for 15 min. After  
162 fixation, cells were permeabilized with the permeation buffer solution for 15 min and washed again.  
163 A reaction mixture was applied to label incorporated EdU, and cells were incubated for 30 min.  
164 Lastly, fluorescent signals were visualized with a DSY2000X inverted fluorescence microscope  
165 (DP80, Olympus, Tokyo, Japan).

166 **Flow cytometry (FCM) assay.** Apoptosis was assessed using Annexin V-fluorescein  
167 isothiocyanate (FITC) and propidium iodide (PI) double staining. Cells were collected, centrifuged  
168 at  $800 \times g$ , and the supernatant was removed. Afterward, the cell pellet was resuspended using the  
169 Annexin V-FITC apoptosis detection kit (BD Biosciences, San Jose, CA, USA) based on the  
170 provided protocols, followed by the addition of 5  $\mu$ l FITC and 5  $\mu$ l PI in the dark. Finally, apoptotic  
171 cells were quantified using a BD FACSCalibur flow cytometer (MoFloAstrios EQ, Beckman  
172 Coulter, CA, USA).

173 **Experimental animals.** BALB/c nude mice (equal numbers of males and females; weighing 18-20  
174 g) were purchased from Shaanxi Shanyao Medical Biotechnology Co., Ltd. (Xi'an, China). The  
175 mice were housed under a sterile environment at 26-28 °C with a relative humidity of 40-60%, *ad*  
176 *libitum* access to food and water, and a 12 h light/dark cycle.

177 **Animal treatment and grouping.** To induce *in vivo* tumor formation,  $2 \times 10^6$  PC3 cells were  
178 subcutaneously injected into the right axillary region of the forelimb of nude mice. Tumor volume  
179 was measured with a vernier caliper, and grouping treatment was initiated when tumors reached 50  
180  $\text{mm}^3$ . After tumor establishment *in vivo*, the nude mice were randomly assigned to three groups  
181 ( $n=6$  mice/group): 1) the PCa group: tumorigenesis was induced in nude mice by injection of PC3  
182 cells, and an equal dose of phosphate-buffered saline (PBS) was injected into mice without miRNA  
183 treatment; 2) the agomir miR-5681b group: tumor-bearing mice were injected with agomir  
184 miR-5681b; and 3) the agomir NC group: tumor-bearing mice were injected with negative control  
185 agomir NC. Each nude mouse received intratumoral multipoint injection of 3 nmol of agomir

186 miR-5681b (HY-R01760A, MCE) or agomir NC (HY-R04602A, MCE) every two days over a  
187 two-week period, with a total of 7 injections (21 nmol). Twenty-four hours after completion of all  
188 interventions, tumor tissues were harvested. A portion of the tumor tissues from each group was  
189 fixed in 4% paraformaldehyde (Solarbio) for 24 h, dehydrated in ethanol, cleared in xylene,  
190 embedded in paraffin, and sectioned at 5  $\mu$ m thickness. Sections were deparaffinized and hydrated  
191 for immunofluorescence. The remaining tumor tissues were prepared into tissue homogenates for  
192 western blot, RT-qPCR, and kit detection.

193 All animal experiments were reviewed and approved by the Institutional Animal Care and Use  
194 Committee of The First Affiliated Hospital of Xi'an JiaoTong University Yulin Hospital (Approval  
195 No. 2025-085). Significant efforts were made in order to minimize both the number of animals  
196 used and their respective suffering.

197 **Terminal deoxynucleotidyl transferase-mediated dUTP nick end-labeling (TUNEL) staining.**

198 Tumor tissue sections were incubated with Protease K working solution (Sigma-Aldrich, St. Louis,  
199 MO, USA) for 22 min at 37 °C before three PBS washes. Tissue paraffin sections were treated with  
200 0.1% triton for 20 min. Subsequent to PBS washing, the sections were added dropwise with buffer  
201 and incubated for 10 min at ambient temperature. The appropriate amounts of TdTase, dUTP, and  
202 buffer were mixed at a ratio of 1:5:50 following the instructions of the TUNEL staining kit (T2196,  
203 Solarbio) and incubated with the sections at 37 °C for 2 h, followed by PBS washing. DAPI  
204 staining solution was added dropwise for 10 min section incubation at room temperature in the dark.  
205 After being blocked with anti-fluorescence quenching agents, the sections were observed and  
206 photographed under a confocal fluorescence microscope (DMI8, Leica, Wetzlar, Germany).

207 **Immunohistochemistry (IHC).** Tumor tissue sections were subjected to antigen retrieval through  
208 boiling in 0.01 M sodium citrate buffer (Sigma-Aldrich), followed by incubation with 3% H<sub>2</sub>O<sub>2</sub> at  
209 room temperature for 15 min. Sections were then blocked with 5% goat serum (Solarbio) for 30  
210 min and incubated overnight at 4 °C with anti-Ki-67 primary antibodies (0.5  $\mu$ g/ml, #ab15580,  
211 Abcam). Afterward, the sections were incubated with horseradish peroxidase (HRP)-conjugated  
212 immunoglobulin G (IgG) H&L secondary antibodies (1:1000, #ab6721, Abcam) at room  
213 temperature for 2 h. Visualization was performed using 3,3-diaminobenzidine (Solarbio), followed  
214 by section counterstaining and mounting. After that, the sections were examined and photographed

215 under a light microscope, and the percentage of positively stained cells was quantified using  
216 Image-Pro Plus 6.0 (Media Cybernetics, Silver Spring, MD, USA).

217 **Western blot.** Total proteins were extracted from cells using radio-immunoprecipitation assay cell  
218 lysis buffer (Beyotime Biotechnology, Shanghai, China). Protein concentrations were determined  
219 using a bicinchoninic acid protein detection kit (Rockford, IL, USA). Afterward, 30  $\mu\text{g}$ /well of the  
220 protein sample was loaded onto a 10% or 12% sodium dodecyl sulfate-polyacrylamide gel  
221 electrophoresis. Subsequently, the proteins were transferred to a polyvinylidene fluoride (PVDF)  
222 membrane. After being blocked with 5% skim milk for 2 h, the PVDF membrane was cultured in  
223 the presence of primary antibodies against rabbit anti-Bcl-1 (1/2000, #ab207612, Abcam) [26],  
224 rabbit anti-Cleaved Caspase-1 (1/500, #ab32042, Abcam) [27], rabbit anti-B-cell lymphoma 2  
225 (Bcl-2)-associated X protein (Bax) (1/1000, #ab32503, Abcam) [28], rabbit anti-Bcl-2 (1/2000,  
226 #ab182858, Abcam) [29], rabbit anti-light chain-3B (LC3B) (1/3000, #ab51520, Abcam) [30],  
227 rabbit anti-P62 (1/10000, #ab109012, Abcam) [31], and rabbit anti- $\beta$ -actin (1/1000, #ab8226,  
228 Abcam) [32] overnight at 4 °C. After being rinsed thrice with Tris-buffered saline with Tween-20,  
229 the membranes were incubated with HRP-labeled goat anti-rabbit IgG H&L (1:5000, #ab6721,  
230 Abcam) [33] for 1 h at room temperature, followed by visualization using enhanced  
231 chemiluminescence working solution (EMD Millipore, Billerica, MA, USA). The quantification of  
232 proteins was conducted utilizing Image Pro Plus 6.0 software (Media Cybernetics).  $\beta$ -actin served  
233 as an internal reference. Additionally, the linear range of  $\beta$ -actin was assessed using different total  
234 protein contents, following the methodology described in a previous study [34]. The results showed  
235 that  $\beta$ -actin levels exhibited no significant variation when the protein content exceeded 4  $\mu\text{g}$ ,  
236 indicating protein overload. Therefore, in this study, 3  $\mu\text{g}$  of protein samples were loaded for  
237 western blot to ensure that the internal reference protein signal was maintained within the effective  
238 linear range (Supplementary Figure S1).

239 **Statistical analysis.** Statistical analyses and plotting were performed using GraphPad Prism 9.5.0  
240 software (GraphPad Software Inc., San Diego, CA, USA). The Shapiro-Wilk test was employed to  
241 assess the normal distribution of data. Normally distributed measurement data were presented as  
242 mean $\pm$ standard deviation and compared between two groups using the independent sample *t* test.

243 One-way analysis of variance (ANOVA) was applied for multi-group comparisons, followed by  
244 Tukey's test.  $P < 0.05$  was indicative of significant differences.

245

## 246 **Results**

247 **miR-5681b expression is decreased in PCa cell lines and can target Beclin-1.** The differential  
248 miRNAs of PCa patients were screened from the dbDMED database using the filter criteria of  
249  $\text{LogFC} < 2$  and  $\text{FDR} < 0.05$ . A volcano plot (Figure 1A) was generated to visualize downregulated  
250 miRNAs in PCa (Supplementary Table S1). PCa-related miRNAs were obtained from the  
251 Genecards database (Supplementary Table S3). Previous studies have implicated the  
252 autophagy-related gene Beclin-1 in PCa pathogenesis and unveiled its role in inhibiting tumor cell  
253 apoptosis [16, 35]. Subsequently, the upstream miRNA of Beclin-1 was predicted using the  
254 miRanda database (Supplementary Table S2). Finally, the intersection of these results was  
255 determined using Venny 2.1.0 (<https://bioinfo.gp.cnb.csic.es/tools/venny/index.html>), identifying  
256 miR-5681b as an upstream miRNA of Beclin-1, which was significantly downregulated in PCa  
257 (Figure 1B).

258 To investigate miR-5681b expression in PCa cells and its regulatory relationship with Beclin-1, we  
259 cultured RWPE-1 (normal prostate epithelial) and PCa cell lines (LnCaP, DU145, PC3, and 22RV1)  
260 *in vitro*. RT-qPCR data revealed significantly lower miR-5681b expression in PCa cell lines  
261 compared to RWPE-1 (all  $p < 0.05$ , Figure 1C). Accordingly, PC3 and LnCaP cells with relatively  
262 low expression of miR-5681b were selected for the subsequent experiments. The binding sites  
263 between miR-5681b and Beclin-1 were identified using the miRanda database (Figure 1D).  
264 Dual-luciferase assay demonstrated that co-transfection of Beclin-1 wild-type (Beclin-1-WT) and  
265 miR-5681b mimic significantly reduced luciferase activity (all  $p < 0.05$ , Figure 1E), whereas no  
266 significant changes were observed in the luciferase activity of cells treated with Beclin-1-WT and  
267 mimic NC (all  $p > 0.05$ , Figure 1E). Additionally, miR-5681b was overexpressed in PC3 and  
268 LnCaP cells (all  $p < 0.05$ , Figure 1F), which resulted in decreased Beclin-1 mRNA and protein  
269 levels in PC3 and LnCaP cells (all  $p < 0.05$ , Figures 1G, 1H). These findings indicate that  
270 miR-5681b is downregulated in PC3 cells and miR-5681b targets Beclin-1.

271 **miR-5681b inhibits proliferation and facilitates apoptosis in PCa cells.** To explore the role of  
272 miR-5681b in PCa cells, we evaluated cell viability using CCK-8 assay. miR-5681b mimic  
273 significantly reduced cell viability ( $p < 0.05$ , Figure 2A). EdU staining confirmed that miR-5681b  
274 mimic inhibited PCa cell proliferation ( $p < 0.05$ , Figure 2B). Additionally, apoptosis was enhanced  
275 following miR-5681b mimic transfection (all  $p < 0.05$ , Figure 2C). miR-5681b mimic elevated the  
276 expression of cleaved caspase-3 and Bax and lowered Bcl-2 expression (all  $p < 0.05$ , Figure 2D).  
277 These results indicate that miR-5681b suppresses PCa cell proliferation and promotes apoptosis.

278 **Beclin-1 upregulation partially reverses the effects of miR-5681b on PCa cell proliferation  
279 and apoptosis.** To further explore whether miR-5681b regulates proliferation and apoptosis in PCa  
280 cells by targeting Beclin-1, PC3 and LNCaP cells were co-transfected with miR-5681b mimic and  
281 either pcDNA3.1-Beclin-1 or the empty pcDNA3.1 vector. Compared to the miR-5681b  
282 mimic+pcDNA group, the mRNA and protein expression of Beclin-1 were increased in the  
283 miR-5681b mimic+pcDNA-Beclin-1 group (all  $p < 0.05$ , Figures 3A, 3B), accompanied by boosted  
284 cell viability (Figure 3C) and proliferation (Figure 3D) ( $p < 0.05$ ), and reduced apoptosis ( $p < 0.05$ ,  
285 Figure 3E). Meanwhile, the expression of Bax and cleaved caspase-3 in the miR-5681b  
286 mimic+pcDNA-Beclin-1 group decreased as compared to that in the miR-5681b mimic+pcDNA  
287 group, with elevated Bcl-2 expression ( $p < 0.05$ , Figure 3F). These results illustrate that miR-5681b  
288 targets Beclin-1 to suppress proliferation and boost apoptosis in PCa cells, and Beclin-1  
289 overexpression partially reverses these effects.

290 **miR-5681b regulates PCa cell autophagy by targeting Beclin-1.** Beclin-1 is a well-established  
291 gene associated with the process of autophagy [36]. Western blot demonstrated that LC3-I and p62  
292 protein expression was augmented, and LC3-II/LC3-I and LC3-II levels declined after miR-5681b  
293 mimic transfection, while these effects were reversed by Beclin-1 overexpression ( $p < 0.05$ , Figure  
294 4A). In accordance, miR-5681b limits autophagy in PCa cells through the inhibition of Beclin-1  
295 expression.

296 **Activation of autophagy partially abrogates the effect of miR-5681b on PCa cell apoptosis  
297 and proliferation.** We further treated PC3 and LNCaP cells with the autophagy inhibitor 3-MA to  
298 suppress cell autophagy. The results showed that 3-MA markedly reduced the levels of the  
299 autophagy-related protein LC3-II and the LC3-II/LC3-I ratio, while increasing LC3-I and P62

300 protein expression in PC3 and LNCaP cells ( $p < 0.05$ , Figure 5A). In addition, 3-MA treatment  
301 obviously decreased PC3 and LNCaP cell viability ( $p < 0.05$ , Figure 5B) and proliferation ( $p < 0.05$ ,  
302 Figure 5C), while accelerating their apoptosis ( $p < 0.05$ , Figure 6B). Meanwhile, the expression of  
303 Bax and cleaved caspase-3 was prominently augmented, and Bcl-2 expression was lowered in PC3  
304 and LNCaP cells upon 3-MA treatment (all  $p < 0.05$ , Figure 6A). PC3 and LncCaP cells were  
305 subjected to treatment with the autophagy activator Rapamycin, concomitant with the  
306 overexpression of miR-5681b. Compared to the miR-5681b mimic group, the miR-5681b  
307 mimic+Rapamycin group showed elevations in the level of LC3-II and the ratio of LC3-II/LC3-I  
308 and declines in the levels of LC3-I and P62 proteins ( $p < 0.05$ , Figure 5A). Correspondingly, cell  
309 viability ( $p < 0.05$ , Figure 5B) and proliferation ( $p < 0.05$ , Figure 5C) were increased and apoptosis  
310 was attenuated ( $p < 0.05$ , Figure 6B) in the miR-5681b mimic+Rapamycin group when compared  
311 with the miR-5681b mimic group, accompanied by lowered Cleaved caspase-3 and Bax levels and  
312 augmented Bcl-2 levels (all  $p < 0.05$ , Figure 6A). Collectively, these findings highlight that  
313 inhibition of autophagy depresses PCa cell proliferation and potentiates apoptosis, whereas  
314 activation of autophagy partially nullifies the regulatory effects of miR-5681b on proliferation and  
315 apoptosis in PCa cells.

316 **miR-5681b suppresses Beclin-1 to mediate autophagy, thereby inhibiting *in vivo* tumor**  
317 **growth of PCa.** An *in vivo* PCa model was first established by subcutaneously implanting  $2 \times 10^6$   
318 PC3 cells into the right axillary region of nude mice, followed by intratumoral injections of agomir  
319 miR-5681b or agomir NC. The results revealed that agomir miR-5681b treatment significantly  
320 increased miR-5681b expression in tumor tissues ( $p < 0.05$ , Figure 7A), while reducing Beclin-1  
321 expression ( $p < 0.05$ , Figures 7B, 7C). Moreover, agomir miR-5681b markedly enhanced apoptosis  
322 ( $p < 0.05$ , Figure 7D), decreased proliferation ( $p < 0.05$ , Figure 7E) and autophagy ( $p < 0.05$ ,  
323 Figure 7F), and obviously reduced tumor volume and weight ( $p < 0.05$ , Figure 7G). Taken together,  
324 these findings demonstrate that miR-5681b inhibits Beclin-1 mediated autophagy, thereby  
325 suppressing *in vivo* growth of PCa.

326

327 **Discussion**

328 PCa remains the most commonly diagnosed non-cutaneous malignancy in men and is a major cause  
329 of cancer-related mortality worldwide [37]. Although localized PCa has a relatively high long-term  
330 survival rate, metastatic PCa remains largely incurable despite multimodal treatment approaches [7].  
331 Emerging evidence highlights the role of miRNAs in regulating key genes involved in drug  
332 resistance and aggressiveness of PCa [38, 39]. Notably, deletion of a single copy of Beclin-1 has  
333 been reported in 40-75% of PCa cases [40]. Herein, this study aims to elucidate the mechanism by  
334 which miR-5681b regulates the autophagy-related protein Beclin-1, thereby modulating the  
335 proliferation and apoptosis of PCa cells.

336 miRNAs modulate post-transcriptional gene expression by binding to complementary sequences  
337 within the 3'-UTR of target mRNAs, leading to mRNA degradation or translational repression [41].  
338 Approximately 60% of human genes are modulated by miRNAs [42]. Beclin-1 has been implicated  
339 in the initiation and progression of PCa [35]. Not surprisingly, Beclin-1 is also modulated by its  
340 upstream miRNAs, including miR-30a, as previously reported [43]. In this study, bioinformatics  
341 analysis identified miR-5681b as an upstream regulator of Beclin-1, which was downregulated in  
342 PCa. In androgen-independent PCa, several tumor-suppressive miRNAs (like miR-31, miR-148a,  
343 and miR-200b-3p) are downregulated, contributing to tumor aggressiveness, progression, and  
344 resistance to androgen deprivation [39]. Furthermore, we confirmed reduced miR-5681b expression  
345 in PCa cells and validated its targeting on Beclin-1 by RT-qPCR and dual-luciferase assays.  
346 Overexpression of miR-5681b significantly decreased Beclin-1 mRNA and protein expression.  
347 Likewise, miR-30a may target Beclin-1 and suppress autophagy by decreasing Beclin-1 expression  
348 [43]. In conclusion, this study demonstrated for the first time that miR-5681b expression was  
349 reduced in PCa cell lines and that it directly suppressed Beclin-1 expression.

350 PCa is characterized by the dysregulation of multiple miRNAs, which function as either tumor  
351 suppressors or oncogenes [44]. Beclin-1 is a vital autophagy protein, and yeast two-hybrid  
352 screening revealed that it interacts effectively with Bcl-2 [45]. Numerous studies highlight the  
353 critical roles of miRNAs in PCa progression, including effects on proliferation, cell cycle, invasion,  
354 metastasis, and apoptosis, functioning as tumor repressors or oncogenes depending on their target  
355 genes [46-48]. Our results showed that miR-5681b upregulation inhibited viability, proliferation,  
356 and Bcl-2 expression, while promoting apoptosis and increasing cleaved caspase-3 and Bax levels

357 in PCa cells; these effects were partially reversed by Beclin-1 overexpression. Similarly, miR-92a  
358 overexpression suppresses PCa cell invasion, viability, and migration [49]. miR-340 also reduces  
359 invasiveness, proliferation, and migration, while driving apoptosis in PCa cells [50]. Additionally,  
360 overexpressed miR-106a promotes apoptosis and inhibits proliferation, migration, and invasion by  
361 directly targeting IL-8 in PCa cells [51]. Zhang et al. have reported that elevated miR-216a  
362 expression suppresses PCa cell proliferation and accelerates cell apoptosis, whereas Beclin-1  
363 overexpression negates the effects of miR-216a [52]. To our knowledge, our study is the first study  
364 to describe the role of miR-5681b on PCa progression. Briefly, miR-5681b suppresses PCa cell  
365 proliferation and induces apoptosis, which is partially abrogated by Beclin-1 upregulation.  
366 Autophagy plays a critical role in promoting the survival and proliferation of PCa cells [14]. LC3 is  
367 commonly utilized as a biomarker for autophagy because of its strong correlation with  
368 autophagosome abundance, marked by the conversion of LC3-I to LC3-II [53]. p62 is a selective  
369 autophagy receptor involved in multiple pathways and is ubiquitously expressed in cells [54].  
370 Interestingly, p62/SQSTM1 accumulation, an autophagy receptor, is positively correlated with  
371 LC3-II elevation [55]. In our study, co-overexpression of miR-5681b and Beclin-1 diminished  
372 LC3-I and p62 protein expression and elevated LC3-II/LC3-I and LC3-II levels. Consistently,  
373 miR-146b has been reported to inhibit autophagy in PCa via the PTEN/Akt/mTOR pathway [56].  
374 Furthermore, miR-30a is well documented to directly target Beclin-1 in cancer cells [43]. As  
375 reported, the PI3K/Akt/mTOR pathway can be activated by downregulating Beclin-1 in lung cancer  
376 cells [57]. However, mTOR inhibitors may prevent the reduction of Beclin-1 [58], and artesunate  
377 induces Beclin-1-mediated autophagy through the suppression of mTOR signaling [59]. Overall,  
378 miR-5681b can suppress PCa cell autophagy through targeted repression of Beclin-1.  
379 Tumor growth can be promoted or inhibited through the regulation of immune cell homeostasis,  
380 activation, proliferation, and differentiation by activating autophagy [60]. The autophagy activator  
381 Rapamycin was employed in the treatment of PC3 cells with simultaneous overexpression of  
382 miR-5681b. Our results demonstrated that autophagy activation stimulated PCa cell proliferation  
383 and inhibited apoptosis. Consistent with these findings, Rapamycin has been shown to induce  
384 autophagy in human neuroblastoma cells, as evidenced by elevated levels of LC3-II, LC3-II/LC3-I,  
385 and Beclin-1 and diminished levels of p62 [61]. PCa cell proliferation can be increased by

386 activating autophagy before treatment with olaparib [62]. In addition, treatment with Rapamycin  
387 restores autophagy and suppresses mTORC1-mediated apoptosis in cancer cells, with its  
388 anti-apoptotic effects linked to reduced p62 levels [63]. Taken together, the effects of miR-5681b  
389 on PCa cell apoptosis and proliferation can be partially reversed by autophagy activation. Our  
390 xenograft tumor experiments in nude mice also confirmed that miR-5681b inhibited Beclin-1 to  
391 regulate autophagy, thereby affecting the *in vivo* growth of PCa.

392 In conclusion, this study elucidates the mechanism of miR-5681b in regulating autophagy-related  
393 protein Beclin-1 and then affecting PCa cell proliferation and apoptosis. Bioinformatics and  
394 literature analyses identified miR-5681b as a significantly downregulated upstream regulator of  
395 Beclin-1 in PCa. Overexpression of miR-5681b suppressed autophagy by targeting Beclin-1,  
396 thereby inhibiting proliferation and accelerating apoptosis in PCa cells. Nevertheless, several  
397 limitations of this study should be acknowledged. On the one hand, currently, no studies have  
398 reported an association between miR-5681b and PCa. However, this study for the first time  
399 demonstrated that miR-5681b expression was significantly downregulated in PCa cells.  
400 Overexpression of miR-5681b repressed cell autophagy by targeting and suppressing Beclin-1,  
401 thereby protecting against the growth of PCa. Additionally, previous studies have unveiled that  
402 miR-21 serves as a potential biomarker for PCa and plays a critical role in PCa cell migration and  
403 proliferation [64, 65]. In addition to miR-21, miR-1246 also functions as a biomarker for PCa and  
404 is closely associated with higher pathological grade, positive metastasis, and poor prognosis of PCa  
405 [66]. These results imply that low miR-5681b expression may be related to the occurrence,  
406 progression, and prognosis of PCa. Future studies will further explore whether miR-5681b could  
407 serve as a potential biomarker for the occurrence and prognosis of PCa at the clinical level. On the  
408 other hand, additional investigation is required to analyze the upstream targets of miR-5681b. In the  
409 future, more comprehensive studies will be conducted to elucidate the regulatory mechanism  
410 underlying PCa involving miR-5681b.

411

412 Acknowledgements: The study was financed under the provisions of the institutional budget.

413

414 **Supplementary data are available in the online version of the paper.**

415

416

417 **References**

- 418 [1] SIEGEL RL, MILLER KD, WAGLE NS, JEMAL A. Cancer statistics, 2023. *CA Cancer J*  
419 *Clin* 2023; 73: 17-48. <https://doi.org/10.3322/caac.21763>
- 420 [2] FENG F, ZHONG YX, CHEN Y, LIN FX, HUANG JH et al. Establishment and validation  
421 of serum lipid-based nomogram for predicting the risk of prostate cancer. *BMC Urol* 2023;  
422 23: 120. <https://doi.org/10.1186/s12894-023-01291-w>
- 423 [3] GROZESCU T, POPA F. Prostate cancer between prognosis and adequate/proper therapy. *J*  
424 *Med Life* 2017; 10: 5-12.
- 425 [4] SHEN MM, ABATE-SHEN C. Molecular genetics of prostate cancer: new prospects for old  
426 challenges. *Genes Dev* 2010; 24: 1967-2000. <https://doi.org/10.1101/gad.1965810>
- 427 [5] TAKAYAMA KI. Splicing Factors Have an Essential Role in Prostate Cancer Progression  
428 and Androgen Receptor Signaling. *Biomolecules* 2019; 9: 131.  
429 <https://doi.org/10.3390/biom9040131>
- 430 [6] MUHAMMAD T, SAKHAWAT A, KHAN AA, MA L, GJERSET RA et al. Mesenchymal  
431 stem cell-mediated delivery of therapeutic adenoviral vectors to prostate cancer. *Stem Cell*  
432 *Res Ther* 2019; 10: 190. <https://doi.org/10.1186/s13287-019-1268-z>
- 433 [7] WANG G, ZHAO D, SPRING DJ, DEPINHO RA. Genetics and biology of prostate cancer.  
434 *Genes Dev* 2018; 32: 1105-1140. <https://doi.org/10.1101/gad.315739.118>
- 435 [8] LI X, HE S, MA B. Autophagy and autophagy-related proteins in cancer. *Mol Cancer* 2020;  
436 19: 12. <https://doi.org/10.1186/s12943-020-1138-4>
- 437 [9] BUCHSER WJ, LASKOW TC, PAVLIK PJ, LIN HM, LOTZE MT. Cell-mediated  
438 autophagy promotes cancer cell survival. *Cancer Res* 2012; 72: 2970-2979.  
439 <https://doi.org/10.1158/0008-5472.CAN-11-3396>
- 440 [10] XU HD, QIN ZH. Beclin 1, Bcl-2 and Autophagy. *Adv Exp Med Biol* 2019; 1206: 109-126.  
441 [https://doi.org/10.1007/978-981-15-0602-4\\_5](https://doi.org/10.1007/978-981-15-0602-4_5)
- 442 [11] WANG S, DENG Z, MA Y, JIN J, QI F et al. The Role of Autophagy and Mitophagy in  
443 Bone Metabolic Disorders. *Int J Biol Sci* 2020; 16: 2675-2691.  
444 <https://doi.org/10.7150/ijbs.46627>
- 445 [12] RAKESH R, PRIYADHARSHINI LC, SAKTHIVEL KM, RASMI RR. Role and regulation  
446 of autophagy in cancer. *Biochim Biophys Acta Mol Basis Dis* 2022; 1868: 166400.  
447 <https://doi.org/10.1016/j.bbadis.2022.166400>
- 448 [13] KMA L, BARUAH TJ. The interplay of ROS and the PI3K/Akt pathway in autophagy  
449 regulation. *Biotechnol Appl Biochem* 2022; 69: 248-264. <https://doi.org/10.1002/bab.2104>
- 450 [14] ASHRAFIZADEH M, PASKEH MDA, MIRZAEI S, GHOLAMI MH, ZARRABI A et al.  
451 Targeting autophagy in prostate cancer: preclinical and clinical evidence for therapeutic  
452 response. *J Exp Clin Cancer Res* 2022; 41: 105.  
453 <https://doi.org/10.1186/s13046-022-02293-6>
- 454 [15] HUANG T, WAN X, ALVAREZ AA, JAMES CD, SONG X et al. MIR93 (microRNA -93)  
455 regulates tumorigenicity and therapy response of glioblastoma by targeting autophagy.  
456 *Autophagy* 2019; 15: 1100-1111. <https://doi.org/10.1080/15548627.2019.1569947>

- 457 [16] LIU R, ZHANG S, WAN R, DENG J, FANG W. Effect of Beclin-1 gene silencing on  
458 autophagy and apoptosis of the prostatic hyperplasia epithelial cells. *Clinics (Sao Paulo)*  
459 2022; 77: 100076. <https://doi.org/10.1016/j.clinsp.2022.100076>
- 460 [17] SALIMINEJAD K, KHORRAM KHORSHID HR, SOLEYMANI FARD S, GHAFFARI  
461 SH. An overview of microRNAs: Biology, functions, therapeutics, and analysis methods. *J*  
462 *Cell Physiol* 2019; 234: 5451-5465. <https://doi.org/10.1002/jcp.27486>
- 463 [18] MOHR AM, MOTT JL. Overview of microRNA biology. *Semin Liver Dis* 2015; 35: 3-11.  
464 <https://doi.org/10.1055/s-0034-1397344>
- 465 [19] STAFFORD MYC, WILLOUGHBY CE, WALSH CP, MCKENNA DJ. Prognostic value of  
466 miR-21 for prostate cancer: a systematic review and meta-analysis. *Biosci Rep* 2022; 42:  
467 BSR20211972. <https://doi.org/10.1042/BSR20211972>
- 468 [20] LI WJ, LIU X, DOUGHERTY EM, TANG DG. MicroRNA-34a, Prostate Cancer Stem  
469 Cells, and Therapeutic Development. *Cancers (Basel)* 2022; 14: 4538.  
470 <https://doi.org/10.3390/cancers14184538>
- 471 [21] LI Q, XU K, TIAN J, LU Z, PU J. MiR-129-5p/DLX1 signalling axis mediates functions of  
472 prostate cancer during malignant progression. *Andrologia* 2021; 53: e14230.  
473 <https://doi.org/10.1111/and.14230>
- 474 [22] RODOR J, KLIMI E, BROWN SD, KRILIS G, BRAGA L et al. Functional screening  
475 identifies miRNAs with a novel function inhibiting vascular smooth muscle cell  
476 proliferation. *Mol Ther* 2025; 33: 615-630. <https://doi.org/10.1016/j.ymthe.2024.12.037>
- 477 [23] PATRA D, BHAVYA K, RAMPRASAD P, KALIA M, PAL D. Anti-cancer drug molecules  
478 targeting cancer cell cycle and proliferation. *Adv Protein Chem Struct Biol* 2023; 135:  
479 343-395. <https://doi.org/10.1016/bs.apcsb.2022.11.011>
- 480 [24] NIU H, WANG J, LI H, HE P. Rapamycin potentiates cytotoxicity by docetaxel possibly  
481 through downregulation of Survivin in lung cancer cells. *J Exp Clin Cancer Res* 2011; 30:  
482 28. <https://doi.org/10.1186/1756-9966-30-28>
- 483 [25] XIN X, WU M, MENG Q, WANG C, LU Y et al. Long noncoding RNA HULC accelerates  
484 liver cancer by inhibiting PTEN via autophagy cooperation to miR15a. *Mol Cancer* 2018;  
485 17: 94. <https://doi.org/10.1186/s12943-018-0843-8>
- 486 [26] MIRRA S, GARCIA-ARROYO R, DOMÈNECH EB, GAVALDA-NAVARRO A,  
487 HERRERA-UBEDA C et al. CERKL, a retinal dystrophy gene, regulates mitochondrial  
488 function and dynamics in the mammalian retina. *Neurobiol Dis* 2021; 156: 105405.  
489 <https://doi.org/10.1016/j.nbd.2021.105405>
- 490 [27] WANG Y, WANG S, LIU J, LU Y, LI D. Licoricidin enhances gemcitabine-induced  
491 cytotoxicity in osteosarcoma cells by suppressing the Akt and NF-kappaB signal pathways.  
492 *Chem Biol Interact* 2018; 290: 44-51. <https://doi.org/10.1016/j.cbi.2018.05.007>
- 493 [28] YAN Y, NIE Y, PENG C, XING F, JI S et al. The circular RNA hsa\_circ\_0001394 promotes  
494 hepatocellular carcinoma progression by targeting the miR-527/UBE2A axis. *Cell Death*  
495 *Discov* 2022; 8: 81. <https://doi.org/10.1038/s41420-022-00866-0>
- 496 [29] LI X, QI J, XU R, XU S, WANG S et al. ZNF432 suppresses endometrial cancer  
497 progression by promoting UPF1 ubiquitination and inducing apoptosis. *Discov Oncol* 2025;  
498 16: 1095. <https://doi.org/10.1007/s12672-025-02915-3>

- 499 [30] ZHANG L, LI J, CUI L, SHANG J, TIAN F et al. RETRACTED: MicroRNA-30b promotes  
500 lipopolysaccharide-induced inflammatory injury and alleviates autophagy through JNK and  
501 NF-kappaB pathways in HK-2 cells. *Biomed Pharmacother* 2018; 101: 842-851.  
502 <https://doi.org/10.1016/j.biopha.2018.02.085>
- 503 [31] BARTOLOME F, DE LA CUEVA M, PASCUAL C, ANTEQUERA D, FERNANDEZ T et  
504 al. Amyloid beta-induced impairments on mitochondrial dynamics, hippocampal  
505 neurogenesis, and memory are restored by phosphodiesterase 7 inhibition. *Alzheimers Res*  
506 *Ther* 2018; 10: 24. <https://doi.org/10.1186/s13195-018-0352-4>
- 507 [32] WU Q, LIU L, FENG Y, WANG L, LIU X et al. UBR5 promotes migration and invasion of  
508 glioma cells by regulating the ECRG4/NF- $\kappa$ B pathway. *J Biosci* 2022; 47:
- 509 [33] JIANG R, DAI Z, WU J, JI S, SUN Y et al. METTL3 stabilizes HDAC5 mRNA in an  
510 m(6)A-dependent manner to facilitate malignant proliferation of osteosarcoma cells. *Cell*  
511 *Death Discov* 2022; 8: 179. <https://doi.org/10.1038/s41420-022-00926-5>
- 512 [34] TAYLOR SC, POSCH A. The design of a quantitative western blot experiment. *Biomed Res*  
513 *Int* 2014; 2014: 361590. <https://doi.org/10.1155/2014/361590>
- 514 [35] LIU C, XU P, CHEN D, FAN X, XU Y et al. Roles of autophagy-related genes Beclin-1 and  
515 LC3 in the development and progression of prostate cancer and benign prostatic  
516 hyperplasia. *Biomed Rep* 2013; 1: 855-860. <https://doi.org/10.3892/br.2013.171>
- 517 [36] KANG R, ZEH HJ, LOTZE MT, TANG D. The Beclin 1 network regulates autophagy and  
518 apoptosis. *Cell Death Differ* 2011; 18: 571-580. <https://doi.org/10.1038/cdd.2010.191>
- 519 [37] RIZZO A, SANTONI M, MOLLICA V, FIORENTINO M, BRANDI G et al. Microbiota  
520 and prostate cancer. *Semin Cancer Biol* 2022; 86: 1058-1065.  
521 <https://doi.org/10.1016/j.semcancer.2021.09.007>
- 522 [38] LUU HN, LIN HY, SORENSEN KD, OGUNWOBI OO, KUMAR N et al. miRNAs  
523 associated with prostate cancer risk and progression. *BMC Urol* 2017; 17: 18.  
524 <https://doi.org/10.1186/s12894-017-0206-6>
- 525 [39] GUJRATI H, HA S, WANG BD. Deregulated microRNAs Involved in Prostate Cancer  
526 Aggressiveness and Treatment Resistance Mechanisms. *Cancers (Basel)* 2023; 15: 3140.  
527 <https://doi.org/10.3390/cancers15123140>
- 528 [40] AITA VM, LIANG XH, MURTY VV, PINCUS DL, YU W et al. Cloning and genomic  
529 organization of beclin 1, a candidate tumor suppressor gene on chromosome 17q21.  
530 *Genomics* 1999; 59: 59-65. <https://doi.org/10.1006/geno.1999.5851>
- 531 [41] BARTEL DP. MicroRNAs: genomics, biogenesis, mechanism, and function. *Cell* 2004; 116:  
532 281-297. [https://doi.org/10.1016/s0092-8674\(04\)00045-5](https://doi.org/10.1016/s0092-8674(04)00045-5)
- 533 [42] FRIEDMAN RC, FARH KK, BURGE CB, BARTEL DP. Most mammalian mRNAs are  
534 conserved targets of microRNAs. *Genome Res* 2009; 19: 92-105.  
535 <https://doi.org/10.1101/gr.082701.108>
- 536 [43] ZHU H, WU H, LIU X, LI B, CHEN Y et al. Regulation of autophagy by a beclin 1-targeted  
537 microRNA, miR-30a, in cancer cells. *Autophagy* 2009; 5: 816-823.  
538 <https://doi.org/10.4161/auto.9064>
- 539 [44] VANACORE D, BOCCCELLINO M, ROSSETTI S, CAVALIERE C, D'ANIELLO C et al.  
540 Micrnas in prostate cancer: an overview. *Oncotarget* 2017; 8: 50240-50251.  
541 <https://doi.org/10.18632/oncotarget.16933>

- 542 [45] HU YJ, ZHONG JT, GONG L, ZHANG SC, ZHOU SH. Autophagy-Related Beclin 1 and  
543 Head and Neck Cancers. *Onco Targets Ther* 2020; 13: 6213-6327.  
544 <https://doi.org/10.2147/OTT.S256072>
- 545 [46] VERDOODT B, NEID M, VOGT M, KUHN V, LIFFERS ST et al. MicroRNA-205, a novel  
546 regulator of the anti-apoptotic protein Bcl2, is downregulated in prostate cancer. *Int J Oncol*  
547 2013; 43: 307-314. <https://doi.org/10.3892/ijo.2013.1915>
- 548 [47] REN D, WANG M, GUO W, HUANG S, WANG Z et al. Double-negative feedback loop  
549 between ZEB2 and miR-145 regulates epithelial-mesenchymal transition and stem cell  
550 properties in prostate cancer cells. *Cell Tissue Res* 2014; 358: 763-778.  
551 <https://doi.org/10.1007/s00441-014-2001-y>
- 552 [48] LEWIS H, LANCE R, TROYER D, BEYDOUN H, HADLEY M et al. miR-888 is an  
553 expressed prostatic secretions-derived microRNA that promotes prostate cell growth and  
554 migration. *Cell Cycle* 2014; 13: 227-239. <https://doi.org/10.4161/cc.26984>
- 555 [49] LIAO G, XIONG H, TANG J, LI Y, LIU Y. MicroRNA-92a Inhibits the Cell Viability and  
556 Metastasis of Prostate Cancer by Targeting SOX4. *Technol Cancer Res Treat* 2020; 19:  
557 1533033820959354. <https://doi.org/10.1177/1533033820959354>
- 558 [50] HUANG K, TANG Y, HE L, DAI Y. MicroRNA-340 inhibits prostate cancer cell  
559 proliferation and metastasis by targeting the MDM2-p53 pathway. *Oncol Rep* 2016; 35:  
560 887-895. <https://doi.org/10.3892/or.2015.4458>
- 561 [51] SHEN P, SUN G, ZHAO P, DAI J, ZHANG X et al. MicroRNA-106a suppresses prostate  
562 cancer proliferation, migration and invasion by targeting tumor-derived IL-8. *Transl Cancer*  
563 *Res* 2020; 9: 3507-3517. <https://doi.org/10.21037/tcr.2020.03.70>
- 564 [52] ZHANG X, SHI H, LIN S, BAM, CUI S. MicroRNA-216a enhances the radiosensitivity of  
565 pancreatic cancer cells by inhibiting beclin-1-mediated autophagy. *Oncol Rep* 2015; 34:  
566 1557-1564. <https://doi.org/10.3892/or.2015.4078>
- 567 [53] MIZUSHIMAN, YOSHIMORI T. How to interpret LC3 immunoblotting. *Autophagy* 2007;  
568 3: 542-545. <https://doi.org/10.4161/auto.4600>
- 569 [54] LIU WJ, YE L, HUANG WF, GUO LJ, XU ZG et al. p62 links the autophagy pathway and  
570 the ubiquitin-proteasome system upon ubiquitinated protein degradation. *Cell Mol Biol Lett*  
571 2016; 21: 29. <https://doi.org/10.1186/s11658-016-0031-z>
- 572 [55] LIEBL MP, MEISTER SC, FREY L, HENDRICH K, KLEMMER A et al. Robust LC3B  
573 lipidation analysis by precisely adjusting autophagic flux. *Sci Rep* 2022; 12: 79.  
574 <https://doi.org/10.1038/s41598-021-03875-8>
- 575 [56] GAO S, ZHAO Z, WU R, WU L, TIAN X et al. MiR-146b inhibits autophagy in prostate  
576 cancer by targeting the PTEN/Akt/mTOR signaling pathway. *Aging (Albany NY)* 2018; 10:  
577 2113-2121. <https://doi.org/10.18632/aging.101534>
- 578 [57] JIAN M, YUNJIA Z, ZHIYING D, YANDUO J, GUOCHENG J. Interleukin 7 receptor  
579 activates PI3K/Akt/mTOR signaling pathway via downregulation of Beclin-1 in lung  
580 cancer. *Mol Carcinog* 2019; 58: 358-365. <https://doi.org/10.1002/mc.22933>
- 581 [58] YANG T, LI D, LIU F, QI L, YAN G et al. Regulation on Beclin-1 expression by mTOR in  
582 CoCl<sub>2</sub>-induced HT22 cell ischemia-reperfusion injury. *Brain Res* 2015; 1614: 60-66.  
583 <https://doi.org/10.1016/j.brainres.2015.04.016>

- 584 [59] WAN Q, CHEN H, XIONG G, JIAO R, LIU Y et al. Artesunate protects against  
585 surgery-induced knee arthrofibrosis by activating Beclin-1-mediated autophagy via  
586 inhibition of mTOR signaling. *Eur J Pharmacol* 2019; 854: 149-158.  
587 <https://doi.org/10.1016/j.ejphar.2019.04.017>
- 588 [60] JIANG GM, TAN Y, WANG H, PENG L, CHEN HT et al. The relationship between  
589 autophagy and the immune system and its applications for tumor immunotherapy. *Mol*  
590 *Cancer* 2019; 18: 17. <https://doi.org/10.1186/s12943-019-0944-z>
- 591 [61] LIN X, HAN L, WENG J, WANG K, CHEN T. Rapamycin inhibits proliferation and  
592 induces autophagy in human neuroblastoma cells. *Biosci Rep* 2018; 38: BSR20181822.  
593 <https://doi.org/10.1042/BSR20181822>
- 594 [62] CAHUZAC M, LANGLOIS P, PEANT B, FLEURY H, MES-MASSON AM et al.  
595 Pre-activation of autophagy impacts response to olaparib in prostate cancer cells. *Commun*  
596 *Biol* 2022; 5: 251. <https://doi.org/10.1038/s42003-022-03210-5>
- 597 [63] VILLAR VH, NGUYEN TL, DELCROIX V, TERES S, BOUCHECAREILH M et al.  
598 mTORC1 inhibition in cancer cells protects from glutaminolysis-mediated apoptosis during  
599 nutrient limitation. *Nat Commun* 2017; 8: 14124. <https://doi.org/10.1038/ncomms14124>
- 600 [64] HAN X, LV C. MiRNA-21 promotes the migration and proliferation of prostate cancer cells  
601 via activating the JAK/STAT pathway. *Discov Oncol* 2025; 16: 162.  
602 <https://doi.org/10.1007/s12672-025-01883-y>
- 603 [65] GUNAWAN RR, ASTUTI I, DANARTO HR. miRNA-21 as High Potential Prostate Cancer  
604 Biomarker in Prostate Cancer Patients in Indonesia. *Asian Pac J Cancer Prev* 2023; 24:  
605 1095-1099. <https://doi.org/10.31557/APJCP.2023.24.3.1095>
- 606 [66] BHAGIRATH D, YANG TL, BUCAY N, SEKHON K, MAJID S et al. microRNA-1246 Is  
607 an Exosomal Biomarker for Aggressive Prostate Cancer. *Cancer Res* 2018; 78: 1833-1844.  
608 <https://doi.org/10.1158/0008-5472.CAN-17-2069>
- 609

## 610 **Figure Legends**

611

612 **Figure 1.** miR-5681b is lowly expressed in PCa cell lines and targets Beclin-1. A-B) miR-5681b  
613 was significantly under-expressed in PCa and showed targeted binding to Beclin-1, with the results  
614 obtained based on bioinformatics informatics combined with literature analysis; C, F) RT-qPCR to  
615 determine the level of miR-5681b in cells; D) The targeted binding sites between Beclin-1 and  
616 miR-5681b were obtained from the miRanda database; E) Dual-luciferase assay; G) RT-qPCR to  
617 measure the mRNA level of Beclin-1 in cells; H) Western blot to determine the level of Beclin-1  
618 protein. All cell experiments were biologically repeated three times (n=3), and all technical tests  
619 were repeated three times. The data were represented by mean±standard deviation, and independent  
620 sample *t*-tests were used for comparisons between the two groups of data in panel E). One-way

621 ANOVA was implemented for inter-group comparisons of data in panels C, F-H), followed by  
622 Tukey's multiple comparison test.  $p < 0.05$  indicated a significant difference

623

624 **Figure 2.** miR-5681b inhibits the proliferation and facilitates apoptosis of PCa cells. A) CCK-8  
625 assay to assess cell viability; B) EdU staining to evaluate cell proliferation; C) FCM assay to assess  
626 cell apoptosis; D) Western blot to determine the levels of cleaved caspase-3, Bax, and Bcl-2  
627 proteins. All cell experiments were biologically repeated three times ( $n=3$ ), and all technical tests  
628 were repeated three times. Data were expressed as mean $\pm$ standard deviation. One-way ANOVA  
629 was used for inter-group comparisons, followed by Tukey's multiple comparison test.  $p < 0.05$   
630 indicated a significant difference

631

632 **Figure 3.** Beclin-1 upregulation partially reverses the effects of miR-5681b on PCa cell  
633 proliferation and apoptosis. A) Beclin-1 mRNA level was determined by RT-qPCR; B, F) The  
634 levels of Beclin-1, Bax, Bcl-2, and cleaved caspase-3 proteins were measured by western blot; C)  
635 Cell viability was assessed by CCK8 assay; D) Cell proliferation was evaluated by EdU staining; E)  
636 Cell apoptosis was assessed by FCM assay. All cell experiments were biologically repeated three  
637 times ( $n=3$ ), and all technical tests were repeated three times. Data were presented as  
638 mean $\pm$ standard deviation. One-way ANOVA was implemented for data comparisons among  
639 multiple groups, and Tukey's multiple comparison test was used for the post-hoc test.  $p < 0.05$   
640 indicated a significant difference

641

642 **Figure 4.** miR-5681b regulates PCa cell autophagy by targeting Beclin-1. Western blot to measure  
643 the levels of autophagy-related proteins LC3-II, LC3-I, and p62. The repetitive cell experiments  
644 were conducted three times. Data were presented as mean $\pm$ standard deviation. One-way ANOVA  
645 was implemented for data comparisons among multiple groups, and Tukey's multiple comparison  
646 test was used for the post-hoc test.  $p < 0.05$  indicated a significant difference.

647

648 **Figure 5.** Activation of autophagy partially averted the regulatory effects of miR-5681b on PCa  
649 cell apoptosis and proliferation. A) The levels of autophagy-related proteins LC3-II, LC3-I, p62

650 were determined by western blot; B) Cell viability was evaluated by CCK-8 assay; C) Cell  
651 proliferation was evaluated by EdU staining; Data were presented as mean±standard deviation.  
652 One-way ANOVA was implemented for data comparisons among multiple groups, followed by  
653 Tukey's multiple comparison test.  $p < 0.05$  indicated a significant difference.

654

655 **Figure 6.** Activation of autophagy partially averted the regulatory effects of miR-5681b on PCa  
656 cell apoptosis and proliferation. A) The levels of apoptosis-related proteins Bax and Bcl-2 were  
657 determined by western blot; B) FCM to assess cell apoptosis. All cell experiments were  
658 biologically repeated three times ( $n=3$ ), and all technical tests were repeated three times. Data were  
659 presented as mean±standard deviation. One-way ANOVA was implemented for data comparisons  
660 among multiple groups, followed by Tukey's multiple comparison test.  $p < 0.05$  indicated a  
661 significant difference

662

663 **Figure 7.** miR-5681b/Beclin-1 regulates autophagy to affects the *in vivo* growth of PCa. A)  
664 RT-qPCR detection of miR-5681b levels in tumor tissues from nude mice; B-C) RT-qPCR and  
665 western blot to measure Beclin-1 levels in tumor tissues from nude mice; D) TUNEL assay for  
666 detecting apoptosis in tumor tissues; E) IHC detection of Ki-67-positive cells to cell proliferation in  
667 tumor tissues; F) Western blot measurement of autophagy-related proteins (LC3-II, LC3-I, and p62)  
668 in tumor tissues; G) Tumor images and weight quantification map. All animal experiments were  
669 performed with six biological replicates ( $n=6$ ), and each technical test was repeated three times.  
670 Data are presented as mean ± standard deviation. Intergroup comparisons were analyzed with  
671 one-way ANOVA, followed by Tukey's multiple comparisons test.  $p < 0.05$  indicated a significant  
672 difference.

673

674 **Table 1.** Primer sequences.

Gene	Forward 5'-3'	Reverse 5'-3'
Beclin1	GGCGGCTCCTATTCCATCAA	TGACCAGGTAAAGCTTAGATGTCA
miR-5681b	GTATTGCCACCCTTTCTAGTC	GTCCAGTTTTTTTTTTTTTTTGAAGAG
U6	CTCGCTTCGGCAGCACA	TTCTTGGGTAGTTTGCAGTT
GAPDH	GATTGTTGCCATCAACGACC	GTGCAGGATGCATTGCTGAC

675

Accepted manuscript

Fig. 1 [Download full resolution image](#)

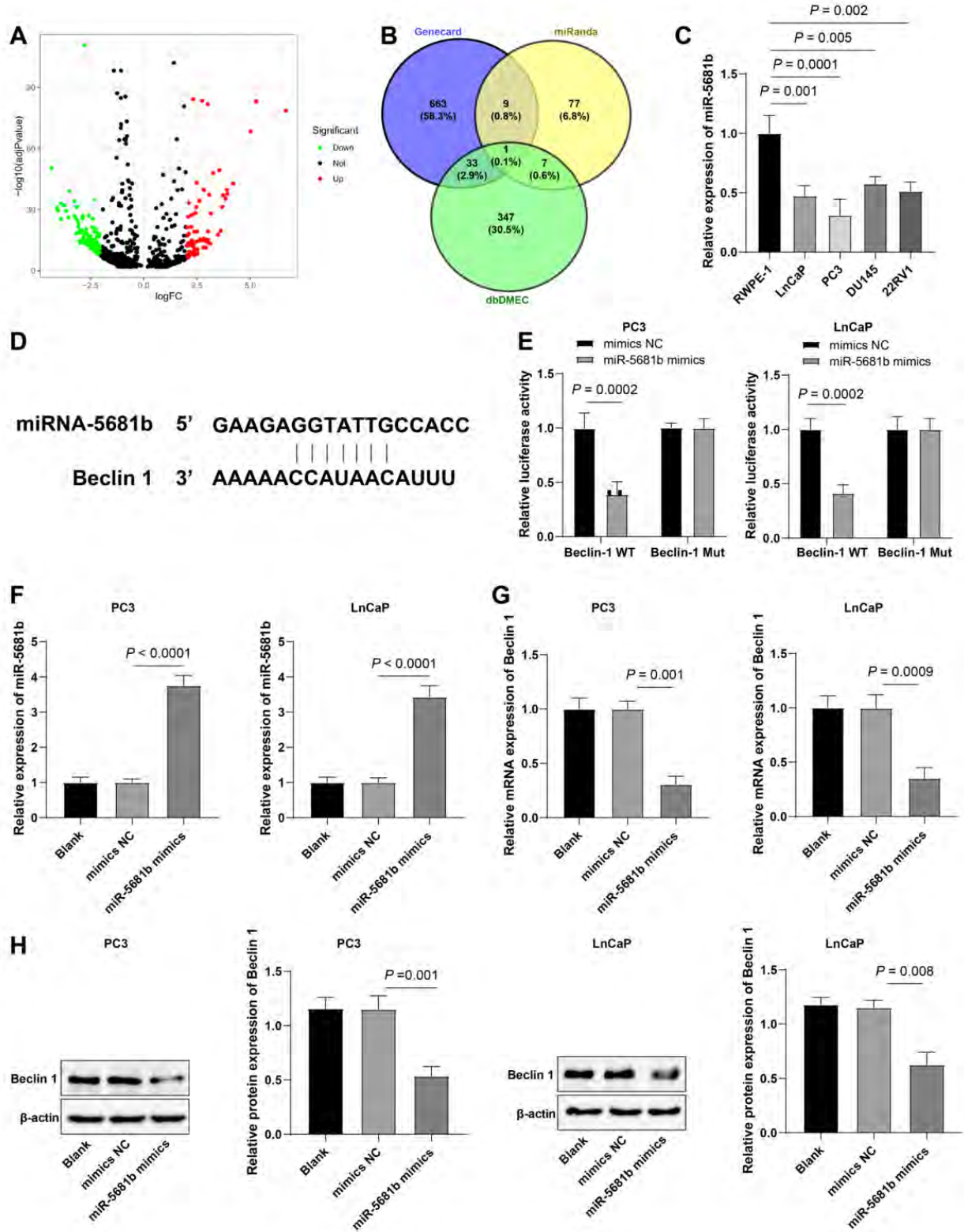


Fig. 2 [Download full resolution image](#)

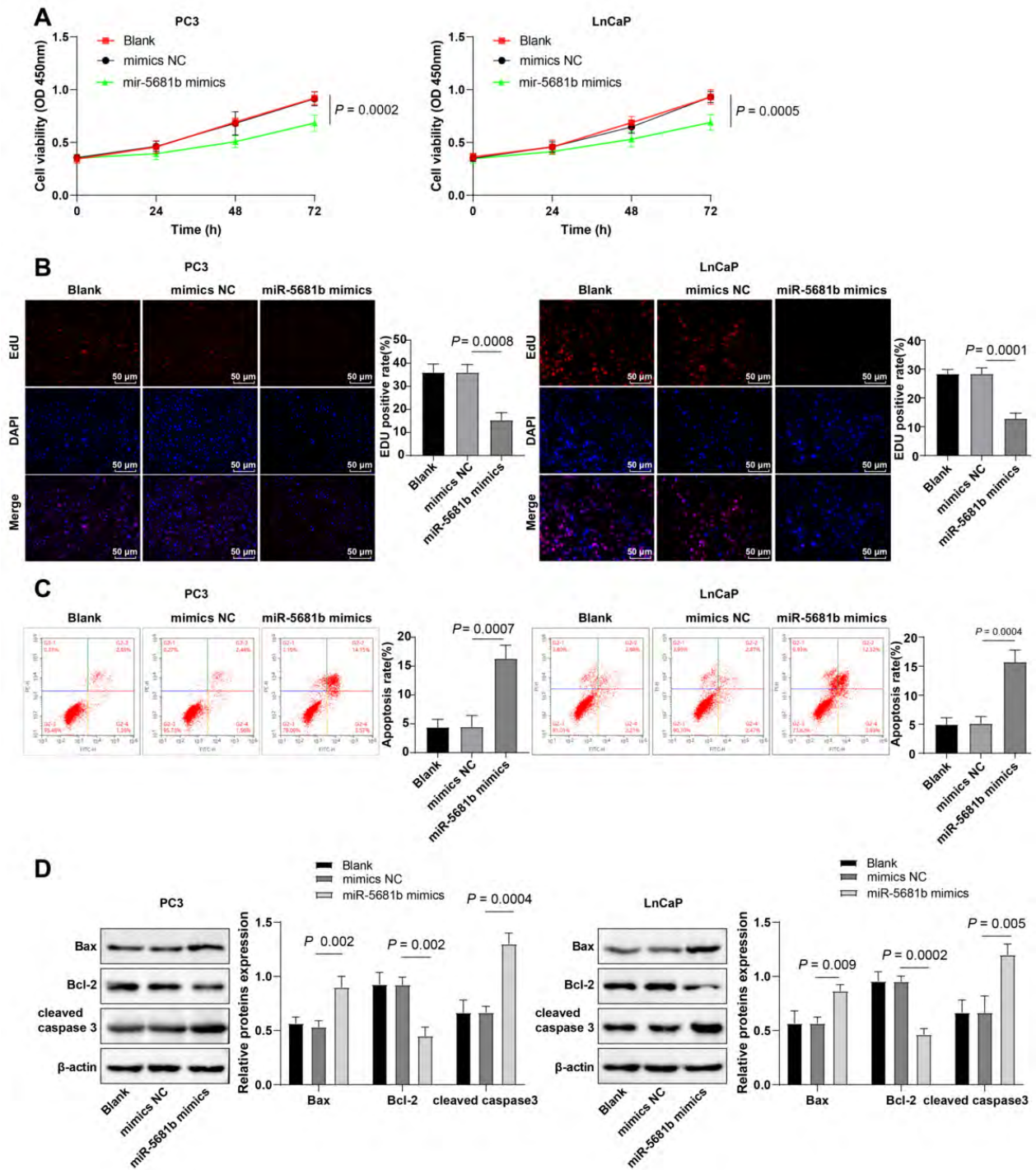


Fig. 3 [Download full resolution image](#)

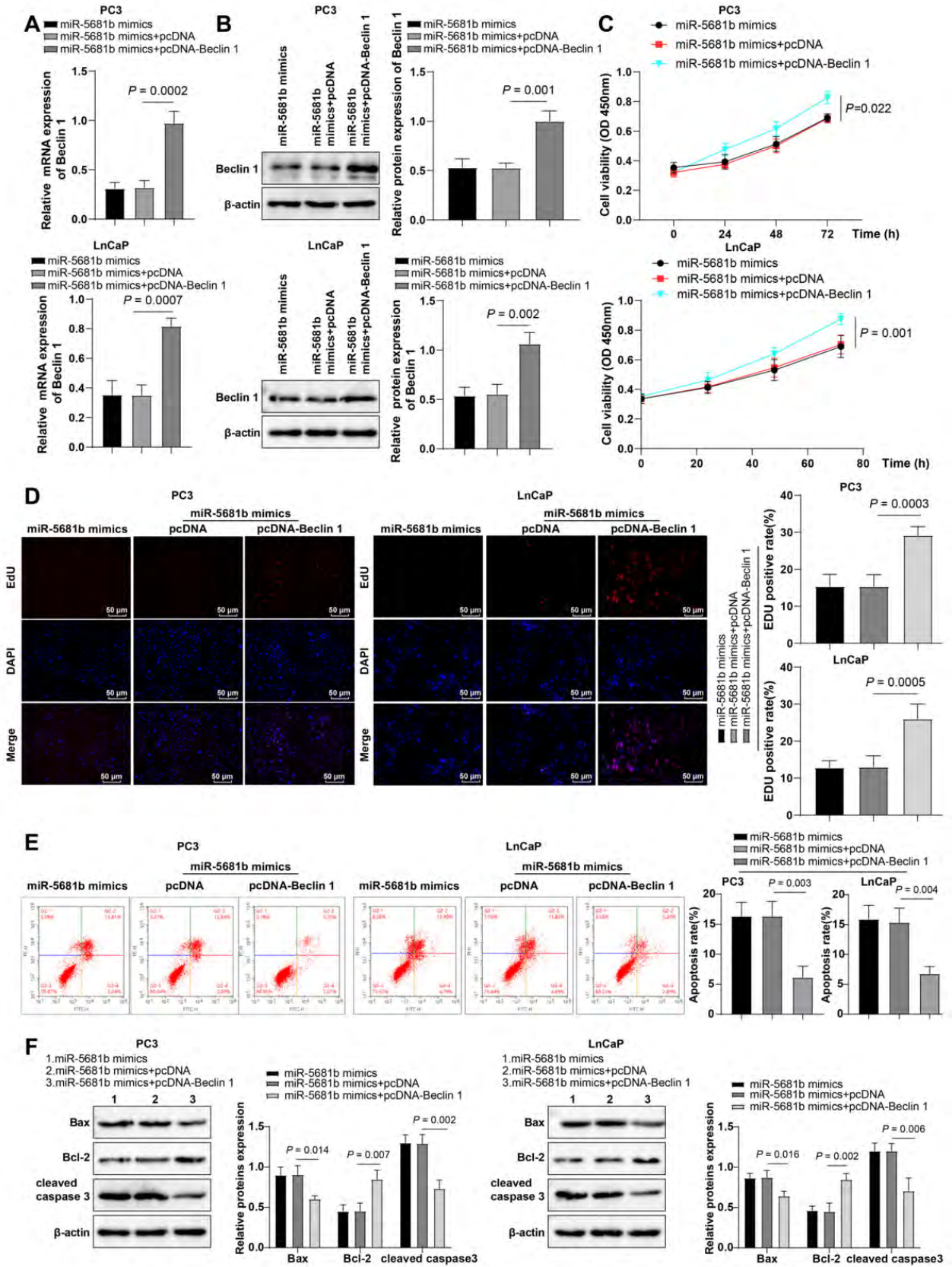


Fig. 4 [Download full resolution image](#)

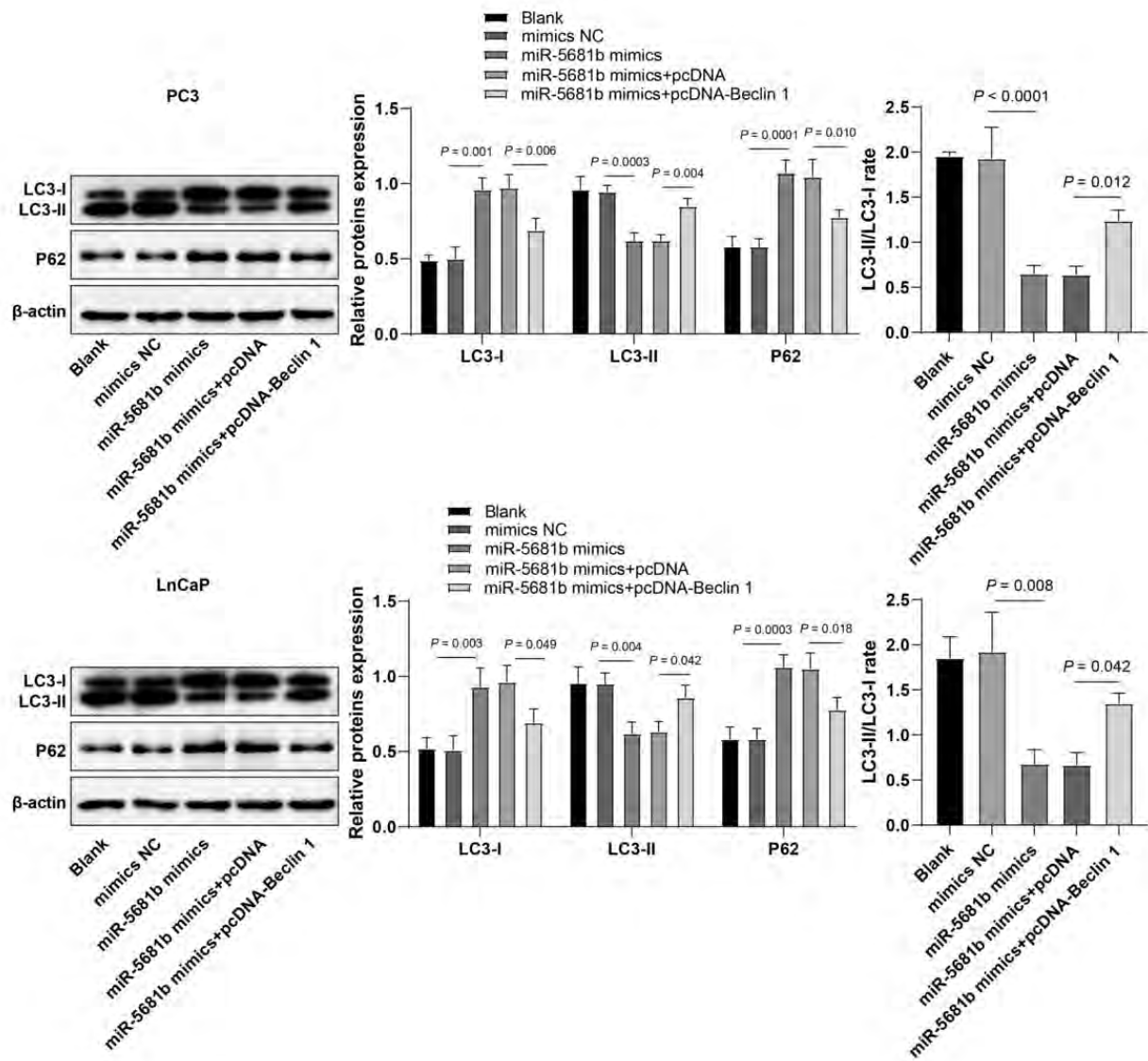


Fig. 5 [Download full resolution image](#)

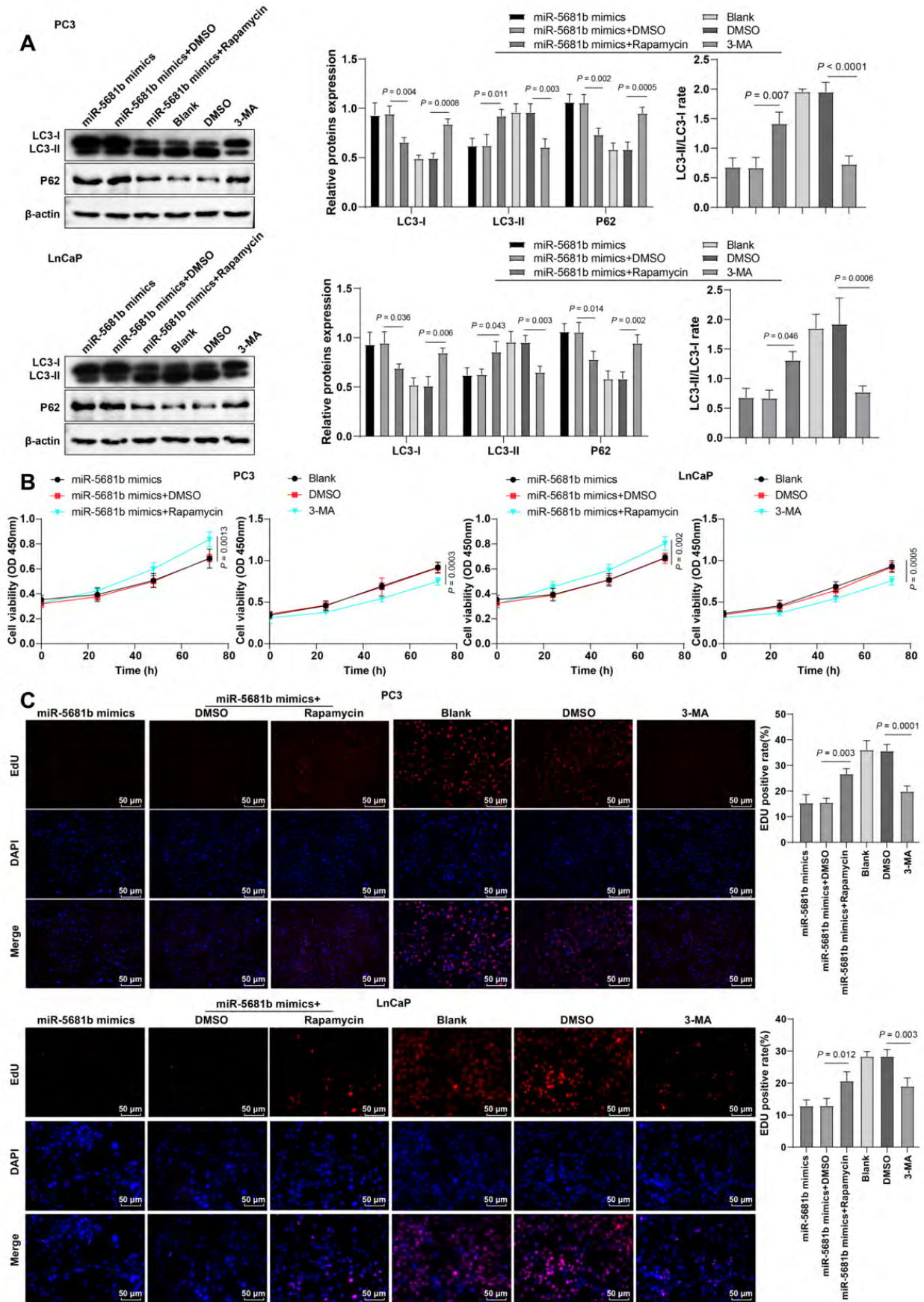


Fig. 6 [Download full resolution image](#)

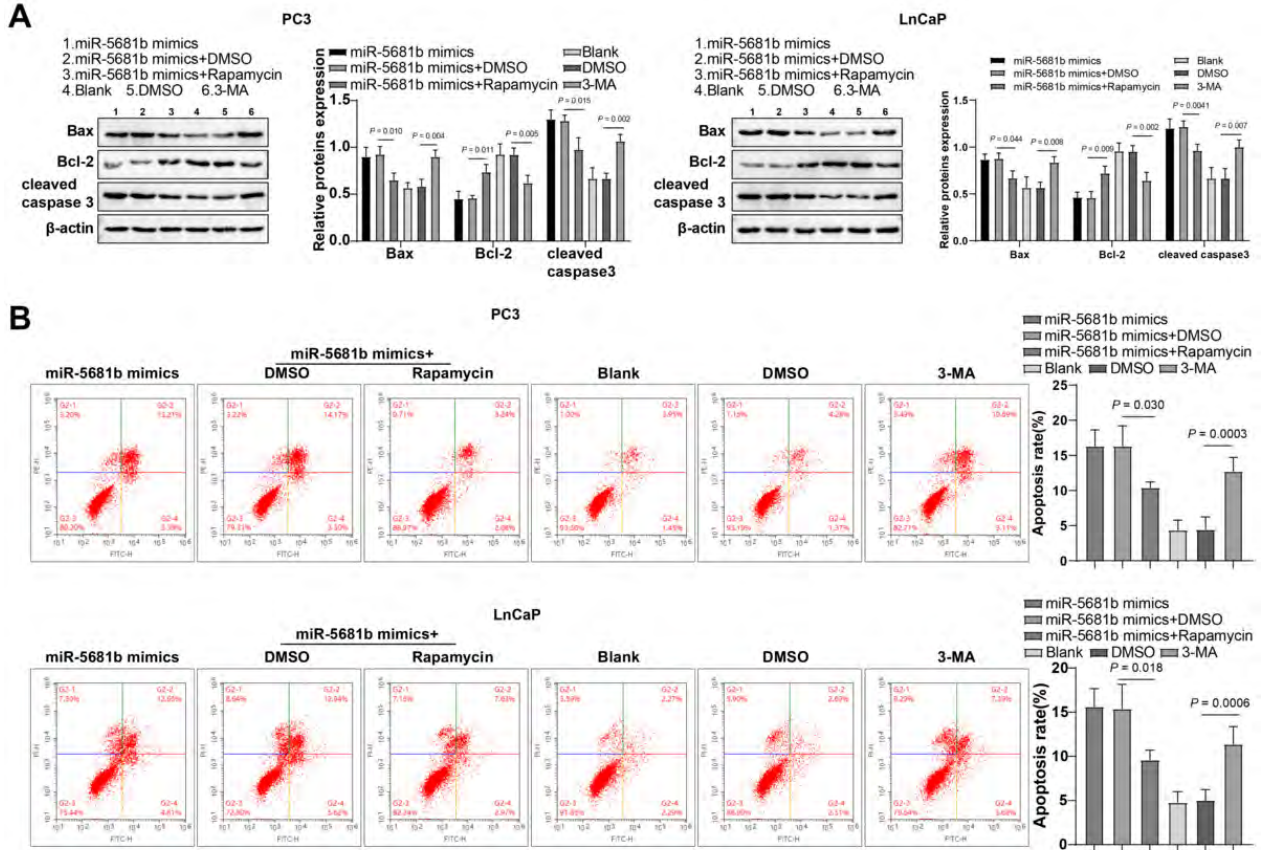


Fig. 7 [Download full resolution image](#)

